

**DEVELOPMENT OF VARIABLE SAMPLING
INTERVAL RUN SUM t CHART AND TRIPLE
SAMPLING \bar{X} CHART WITH ESTIMATED
PROCESS PARAMETERS**

FAIJUN NAHAR MIM

UNIVERSITI SAINS MALAYSIA

2022

**DEVELOPMENT OF VARIABLE SAMPLING
INTERVAL RUN SUM t CHART AND TRIPLE
SAMPLING \bar{X} CHART WITH ESTIMATED
PROCESS PARAMETERS**

by

FAIJUN NAHAR MIM

**Thesis submitted in fulfilment of the requirements
for the degree of
Doctor of Philosophy**

March 2022

ACKNOWLEDGEMENT

Many people have assisted me in completing my Ph.D. thesis successfully and I am genuinely grateful to them. First and foremost, I would like to convey my thanks to my supervisor, Professor Michael Khoo Boon Chong from the School of Mathematical Sciences, Universiti Sains Malaysia (USM), for his unwavering support and encouragement. I am able to successfully complete my Ph.D. studies because of his vast knowledge, extensive experience and profound knowledge on Statistical Quality Control (SQC). I appreciate the time he spent in guiding me, answering my questions, revising and refining the English in my thesis. Without his guidance and relentless help, this thesis would not have been possible. I could not have imagined having a better supervisor in my Ph.D. study.

I am also deeply indebted to the Dean of the School of Mathematical Sciences, USM, Prof. Dr. Hailiza Binti Kamarulhaili, her deputies Assoc. Prof. Dr. Lee See Keong and Assoc. Prof. Dr. Farah Aini, as well as lecturers in the faculty, for their invaluable suggestions and warm-hearted advice. They have encouraged and inspired me to be passionate and enthusiastic about my research. I am thankful to the technical staff of the faculty for their hospitality and technical support. I am also grateful to the USM librarians for all their assistance.

My acknowledgments would be incomplete without thanking my family members, especially my beloved parents and parents-in-law. I managed to complete this thesis successfully because of their unending support and prayers, which has provided a constant source of inspiration to me. I would also like to thank my younger sister and brother for always standing by me. I am greatly indebted to my beloved husband for his enthusiasm and strong support. I also wish to dedicate this thesis to

my beloved sons. Their unwavering support and encouragement is my source of strength.

I wish to extend my gratitude to all my friends for their kindness, help and support during my study. I thank all who have indirectly contributed to the completion of this thesis. Thank you very much. But above all, I would like to thank Allah for all of His help and blessings.

Faijun Nahar Mim

March 2022

TABLE OF CONTENTS

ACKNOWLEDGEMENT	ii
TABLE OF CONTENTS.....	iv
LIST OF TABLES	vii
LIST OF FIGURES	xi
LIST OF ABBREVIATIONS	xiii
LIST OF NOTATIONS	xvi
ABSTRAK.....	xx
ABSTRACT	xxiii
CHAPTER 1 INTRODUCTION.....	1
1.1 Quality and Statistical Process Control	1
1.2 Control Charts.....	3
1.3 Problem Statements	5
1.4 Objectives of the Thesis	7
1.5 Organization of the Thesis.....	7
CHAPTER 2 A REVIEW ON PERFORMANCE MEASURES OF PROPOSED CHARTS, AND RELATED NON-ADAPTIVE AND ADAPTIVE CHARTS.....	10
2.1 Introduction	10
2.2 Performance Measures of Control Charts	11
2.2.1 Average Run Length	12
2.2.2 Average Time to Signal.....	12
2.2.3 Standard Deviation of the Time to Signal.....	13
2.2.4 Average Number of Observations to Signal	13
2.2.5 Average of the Average Run Lengths	14
2.2.6 Standard Deviation of the Average Run Lengths	14
2.2.7 Average of the Average Time to Signal	15
2.2.8 Standard Deviation of the Average Time to Signal.....	15
2.2.9 Average of the Average Number of Observations to Signal	16

2.2.10	Standard Deviation of the Average Number of Observations to Signal .	16
2.3	Run Sum t chart	17
2.4	Some Related Adaptive Type Charts	22
2.4.1	Variable Sampling Interval Exponentially Weighted Moving Average t Chart	29
2.4.2	Double Sampling \bar{X} Chart with Known Process Parameters	32
2.4.3	Two Stage Adaptive Sample Size \bar{X} Chart	37
2.4.4	Three Stage Adaptive Sample Size \bar{X} Chart	39
2.4.5	Triple Sampling \bar{X} Chart with Known Process Parameters	41
2.4.6	Double Sampling \bar{X} Chart with Estimated Process Parameters	47
2.5	Summary.....	51
CHAPTER 3 A PROPOSED KNOWN PROCESS PARAMETER BASED VARIABLE SAMPLING INTERVAL RUN SUM t CHART		52
3.1	Introduction	52
3.2	Operation of the Proposed VSI RS t_K Chart and Computation of Performance Measures	52
3.3	Optimal Design of the Proposed VSI RS t_K Chart	62
3.4	Comparison of Performances of the Proposed VSI RS t_K and Existing t Type Charts	74
3.5	An Example of Application for the Proposed VSI RS t_K Chart.....	81
3.6	Summary.....	86
CHAPTER 4 A PROPOSED ESTIMATED PROCESS PARAMETER BASED VARIABLE SAMPLING INTERVAL RUN SUM t CHART		87
4.1	Introduction	87
4.2	Operation of the Proposed VSI RS t_E Chart and Computation of Performance Measures.....	88
4.3	Optimal Design of the Proposed VSI RS t_E Chart	94
4.4	Performance Analyses of the Proposed VSI RS t_E Chart	97
4.5	An Example of Application for the Proposed VSI RS t_E Chart	110
4.6	Summary.....	113
CHAPTER 5 A KNOWN PROCESS PARAMETERS BASED REVISED TRIPLE SAMPLING \bar{X} CHART		115

5.1	Introduction	115
5.2	Operation and Computation of Performance Measures of the Revised $TS_K \bar{X}$ Chart.....	116
5.3	Optimal Designs of the Revised $TS_K \bar{X}$ Chart	125
5.3.1	Computation of Optimal Parameters in Minimizing $ANOS(\delta)$	125
5.3.2	Computation of Optimal Parameters in Minimizing $ARL(\delta)$	129
5.4	A Performance Comparison between the Revised $TS_K \bar{X}$ and Existing Adaptive Type \bar{X} Charts	131
5.5	An Example of Implementation for the Revised $TS_K \bar{X}$ Chart	134
5.6	Summary.....	139
CHAPTER 6 AN ESTIMATED PROCESS PARAMETERS BASED REVISED TRIPLE SAMPLING \bar{X} CHART		141
6.1	Introduction	141
6.2	Operation of the Revised $TS_E \bar{X}$ Chart and Computation of Performance Measures.....	142
6.3	Optimal Designs of the Revised $TS_E \bar{X}$ Chart.....	156
6.3.1	Computation of Optimal Parameters in Minimizing the $AANOS(\delta)$ Value.....	157
6.3.2	Computation of Optimal Parameters in Minimizing the $AARL(\delta)$ Value	159
6.4	A Performance Comparison between the Revised $TS_E \bar{X}$ and Existing $DS_E \bar{X}$ Charts	161
6.5	An Example of Implementation for the Revised $TS_E \bar{X}$ Chart	170
6.6	Summary.....	174
CHAPTER 7 CONCLUSIONS		176
7.1	Introduction	176
7.2	Contributions and Findings in the Thesis	177
7.3	Suggestions for Future Research.....	182
REFERENCES.....		184
APPENDICES		
LIST OF PUBLICATIONS		

LIST OF TABLES

		Page
Table 2.1	A summary of existing run sum control charts and their descriptions	18
Table 2.2	A summary of existing adaptive type control charts and their descriptions	25
Table 2.3	A summary of the statistics and their distributions used in the 8 steps procedure of the implementation of the $DS_K \bar{X}$ chart	34
Table 2.4	A summary of the statistics and their distributions used in the 11 steps procedure of the $TS_K \bar{X}$ chart.....	44
Table 3.1	Current cumulative scores (at sample i) and next cumulative scores (at sample $i + 1$), for the 4 regions VSI RS t_K chart with scores $\{S_1, S_2, S_3, S_4\}$ $= \{0, 2, 3, 8\}$	60
Table 3.2	Current state (at sample i) to next state (at sample $i + 1$) transitions by regions, for the 4 regions VSI RS t_K chart with scores $\{S_1, S_2, S_3, S_4\} = \{0,$ $2, 3, 8\}$	60
Table 3.3	Complete transition probabilities with thirteen transient states based on Table 3.2.....	61
Table 3.4	Optimal parameter combinations $(M_{(VSI RS t_K)}, t_2, \{S_1, S_2, \dots, S_h\})$ of the VSI RS t_K chart in minimizing the zero-state $ATS(\delta)$ values, for the shift size δ , when $h \in \{4, 7, 10\}$, $t_1 \in \{0.1, 0.3\}$, $G \in \{3, 4\}$, $n = 5$ and $ATS(0) =$ 370	66
Table 3.5	Optimal parameter combinations $(M_{(VSI RS t_K)}, t_2, \{S_1, S_2, \dots, S_h\})$ of the VSI RS t_K chart in minimizing the zero-state $ATS(\delta)$ values, for the shift size δ , when $h \in \{4, 7, 10\}$, $t_1 \in \{0.1, 0.3\}$, $G \in \{3, 4\}$, $n = 7$ and $ATS(0)$ $= 370$	68
Table 3.6	Optimal parameter combinations $(M_{(VSI RS t_K)}, t_2, \{S_1, S_2, \dots, S_h\})$ of the VSI RS t_K chart in minimizing the steady-state $ATS(\delta)$ values, for the shift size δ , when $h \in \{4, 7, 10\}$, $t_1 \in \{0.1, 0.3\}$, $G \in \{3, 4\}$, $n = 5$ and $ATS(0) = 370$	70
Table 3.7	Optimal parameter combinations $(M_{(VSI RS t_K)}, t_2, \{S_1, S_2, \dots, S_h\})$ of the VSI RS t_K chart in minimizing the steady-state $ATS(\delta)$ values, for the shift size δ , when $h \in \{4, 7, 10\}$, $t_1 \in \{0.1, 0.3\}$, $G \in \{3, 4\}$, $n = 7$ and $ATS(0) = 370$	72
Table 3.8	Zero-state $ATS(\delta)$ and $SDTS(\delta)$ values for the VSI RS t_K , RS t and VSI EWMA t charts, when $h \in \{4, 7, 10\}$, $t_1 \in \{0.1, 0.3\}$, $G \in \{3, 4\}$, $n = 5$ and $ATS(0) = 370$	76
Table 3.9	Zero-state $ATS(\delta)$ and $SDTS(\delta)$ values for the VSI RS t_K , RS t and VSI EWMA t charts, when $h \in \{4, 7, 10\}$, $t_1 \in \{0.1, 0.3\}$, $G \in \{3, 4\}$, $n = 7$ and $ATS(0) = 370$	77

Table 3.10	Steady-state $ATS(\delta)$ and $SDTS(\delta)$ values for the VSI RS t_K , RS t and VSI EWMA t charts when $h \in \{4, 7, 10\}$, $t_1 \in \{0.1, 0.3\}$, $G \in \{3, 4\}$, $n = 5$ and $ATS(0) = 370$	78
Table 3.11	Steady-state $ATS(\delta)$ and $SDTS(\delta)$ values for the VSI RS t_K , RS t and VSI EWMA t charts when $h \in \{4, 7, 10\}$, $t_1 \in \{0.1, 0.3\}$, $G \in \{3, 4\}$, $n = 7$ and $ATS(0) = 370$	79
Table 3.12	Phase-I data for the flow width measurements (in microns) of a hard-bake process.....	82
Table 3.13	Phase-II data for the flow width measurements (in microns) of a hard-bake process.....	83
Table 3.14	Summary statistics for the Phase-II data of flow width measurements (in microns) of a hard-bake process	83
Table 4.1	Optimal parameter combinations ($M_{(VSI\ RS\ t_E)}$, t_2 , $\{S_1, S_2, \dots, S_g\}$) of the VSI RS t_E chart in minimizing the zero-state AATS(δ) values, for the shift size δ , when $g \in \{4, 7\}$, $t_1 = 0.1$, $G = 4$, $n = 5$ and $AATS(0) = 370$	98
Table 4.2	Optimal parameter combinations ($M_{(VSI\ RS\ t_E)}$, t_2 , $\{S_1, S_2, \dots, S_g\}$) of the VSI RS t_E chart in minimizing the steady-state AATS(δ) values, for the shift size δ , when $g \in \{4, 7\}$, $t_1 = 0.1$, $G = 4$, $n = 5$ and $AATS(0) = 370$	99
Table 4.3	Optimal parameter combinations ($M_{(VSI\ RS\ t_E)}$, t_2 , $\{S_1, S_2, \dots, S_g\}$) of the VSI RS t_E chart in minimizing the zero-state AATS(δ) values, for the shift size δ , when $g \in \{4, 7\}$, $t_1 = 0.1$, $G = 4$, $n = 7$ and $ATS(0) = 370$	100
Table 4.4	Optimal parameter combinations ($M_{(VSI\ RS\ t_E)}$, t_2 , $\{S_1, S_2, \dots, S_g\}$) of the VSI RS t_E chart in minimizing the steady-state AATS(δ) values, for the shift size δ , when $g \in \{4, 7\}$, $t_1 = 0.1$, $G = 4$, $n = 7$ and $AATS(0) = 370$..	101
Table 4.5	Zero-state AATS(δ) and SDATS(δ) values for the VSI RS t_E chart when $g \in \{4, 7\}$, $t_1 = 0.1$, $G = 4$, $n = 5$ and $AATS(0) = 370$	102
Table 4.6	Steady-state AATS(δ) and SDATS(δ) values for the VSI RS t_E chart when $g \in \{4, 7\}$, $t_0 = 1$, $t_1 = 0.1$, $G = 4$, $n = 5$ and $AATS(0) = 370$	104
Table 4.7	Zero-state AATS(δ) and SDATS(δ) values for the VSI RS t_E chart when $g \in \{4, 7\}$, $t_1 = 0.1$, $G = 4$, $n = 7$ and $AATS(0) = 370$	105
Table 4.8	Steady-state AATS(δ) and SDATS(δ) values for the VSI RS t_E chart when $g \in \{4, 7\}$, $t_1 = 0.1$, $G = 4$, $n = 7$ and $AATS(0) = 370$	106
Table 4.9	Zero-state and steady-state AATS(0) and SDATS(0) values for the VSI RS t_E chart for different number of in-control Phase-I samples (m), computed using the optimal parameters of the VSI RS t_K chart in minimizing $ATS(1.6)$, when $g \in \{4, 7\}$, $t_1 = 0.1$, $G = 4$, $n = 5$ and $ATS(0) = 370$	108

Table 4.10	Zero-state and steady-state AATS(0) and SDATS(0) values for the VSI RS t_E chart for different number of in-control Phase-I samples (m), computed using the optimal parameters of the VSI RS t_K chart in minimizing ATS(1.6), when $g \in \{4, 7\}$, $t_1 = 0.1$, $G = 4$, $n = 7$ and ATS(0) = 370	109
Table 4.11	Summary statistics for the Phase-II data of inside diameter measurements of piston rings (in millimeters)	112
Table 5.1	ARL(0) values of the (i) $TS_K \bar{X}$ chart adopted from He et al. (2002), (ii) revised $TS_K \bar{X}$ chart computed using MATLAB based on the proposed model, (iii) revised $TS_K \bar{X}$ chart simulated using SAS; and the 95% confidence interval for ARL(0) of the $TS_K \bar{X}$ chart simulated using SAS; all obtained based on the parameters in He et al. (2002).....	122
Table 5.2	Optimal parameters $(n_1, n_2, n_3, L_{11}, L_{12}, L_{21}, L_{22}, L_3)$ and the corresponding ANOS(δ) values for the revised $TS_K \bar{X}$ chart, and ANOS(δ) values for the optimal $DS_K \bar{X}$ chart, as well as the percentage of a decrease in the ANOS(δ) value by using the revised $TS_K \bar{X}$ chart in replacing the $DS_K \bar{X}$ chart.....	129
Table 5.3	Optimal parameters $(n_1, n_2, n_3, L_{11}, L_{12}, L_{21}, L_{22}, L_3)$ of the revised $TS_K \bar{X}$ chart in minimizing ARL(δ).....	131
Table 5.4	ARL(δ) values for the revised $TS_K \bar{X}$, $DS_K \bar{X}$, $ASS_3 \bar{X}$ and $ASS_2 \bar{X}$ charts with the percentage of a decrease in the ARL(δ) value by using the revised $TS_K \bar{X}$ chart, in place of an existing chart at hand.....	133
Table 5.5	Phase-I data of the inside diameter measurements (in millimetres) of piston rings	135
Table 5.6	Inside diameter measurements (in millimetres) of piston rings for the Phase-II process monitoring using the revised $TS_K \bar{X}$ chart.....	137
Table 6.1	Optimal parameters $(n_1, n_2, n_3, L_{11}, L_{12}, L_{21}, L_{22}, L_3)$ of the revised $TS_E \bar{X}$ chart when $\tau_5 = 370$, $n \in \{5, 7\}$ and $m \in \{20, 40, 80\}$	158
Table 6.2	AANOS(δ) and SDANOS(δ) values for the optimal revised $TS_E \bar{X}$ and $DS_E \bar{X}$ charts with the percentage of a decrease in the AANOS(δ) value when the revised $TS_E \bar{X}$ chart is used instead of the $DS_E \bar{X}$ chart, based on AANOS(0) = 370, $n \in \{5, 7\}$ and $m \in \{20, 40, 80\}$	160
Table 6.3	Optimal parameters $(n_1, n_2, n_3, L_{11}, L_{12}, L_{21}, L_{22}, L_3)$ of the revised $TS_E \bar{X}$ chart when AARL(0) = 370, $n \in \{5, 7\}$ and $m \in \{20, 40, 80\}$	162
Table 6.4	AARL(δ) and SDARL(δ) values for the optimal revised $TS_E \bar{X}$ and $DS_E \bar{X}$ charts, and the percentage of a decrease in the AARL(δ) value by using the $TS_E \bar{X}$ chart in place of the $DS_E \bar{X}$ chart, based on AARL(0) = 370, $n \in \{5, 7\}$ and $m \in \{20, 40, 80\}$	163

Table 6.5	AANOS(0) and SDANOS(0) values for the revised $TS_E \bar{X}$ chart, for different number of in-control Phase-I samples (m), computed using the optimal parameters of the revised $TS_K \bar{X}$ chart in minimizing ANOS(1.5), based on $n \in \{5, 7\}$ and $ANOS(0) \in \{200, 370\}$	167
Table 6.6	AARL(0) and SDARL(0) values for the revised $TS_E \bar{X}$ chart for different number of in-control Phase-I samples (m), computed using the optimal parameters of the revised $TS_K \bar{X}$ chart in minimizing ARL(1.5), based on $n \in \{5, 7\}$ and $ARL(0) \in \{200, 370\}$	169
Table 6.7	Flow width measurements (in microns) for the Phase-II hard bake process for an implementation of the revised $TS_E \bar{X}$ chart	173

LIST OF FIGURES

		Page
Figure 2.1	A graphical representation of the two-sided RS t chart with a regions, each above and below the CL.....	20
Figure 2.2	A graphical representation of the VSI EWMA t chart's operation ...	32
Figure 2.3	A graphical display of the $DS_K \bar{X}$ chart's operation	33
Figure 2.4	A flow chart explaining the $DS_K \bar{X}$ chart's implementation	35
Figure 2.5	A graphical view of the two-stage adaptive sample size (ASS_2) \bar{X} chart's operation.....	37
Figure 2.6	A graphical view of the three-stage adaptive sample size (ASS_3) \bar{X} chart's operation.....	41
Figure 2.7	A graphical display of the $TS_K \bar{X}$ chart's operation.....	43
Figure 2.8	A flow chart explaining the operation of the $TS_K \bar{X}$ chart	45
Figure 3.1	A graphical representation of the h regions (each above and below the CL) VSI RS t_K chart with the corresponding scores and probabilities of the regions	53
Figure 3.2	Implementation procedure of the VSI RS t_K chart.....	57
Figure 3.3	A flow chart for computing the optimal parameters and score combination of the VSI RS t_K chart in minimizing $ATS(\delta)$	64
Figure 3.4	VSI RS t_K chart for the flow width measurements of a hard bake process.....	85
Figure 4.1	A graphical representation of the g regions VSI RS t_E chart with their corresponding scores and probabilities	90
Figure 4.2	A flow chart for computing the optimal parameters of the VSI RS t_E chart in minimizing the $AATS(\delta)$ value.....	96
Figure 4.3	VSI RS t_E chart for the Phase-II data of inside diameter measurements of piston rings	113
Figure 5.1	A flow chart for the optimization procedure of the revised $TS_K \bar{X}$ chart in minimizing the value of $ANOS(\delta)$	128
Figure 5.2	A flow chart explaining the operation of the revised $TS_K \bar{X}$ chart in monitoring the Phase-II process	136

Figure 5.3	Revised $TS_K \bar{X}$ chart for monitoring of the inside diameter measurements (in millimetres) of piston rings in the Phase-II process	139
Figure 6.1	A flow chart explaining the operation of the revised $TS_E \bar{X}$ chart for the Phase-II process, for monitoring of flow width measurements (in microns) from the hard bake process	172
Figure 6.2	Revised $TS_E \bar{X}$ chart for the Phase-II process for monitoring of flow width measurements (in microns) from the hard bake process	174

LIST OF ABBREVIATIONS

ARL	Average run length
ARL(0)	In-control average run length
ARL(δ)	Out-of-control average run length
EAARL	Expected average of the average run lengths
EARL	Expected average run length
AARL	Average of the average run lengths
AARL(0)	In-control average of the average run lengths
AARL(δ)	Out-of-control average of the average run lengths
SDRL	Standard deviation of the run length
SDARL	Standard deviation of the average run lengths
SDARL(0)	In-control standard deviation of the average run lengths
SDARL(δ)	Out-of-control standard deviation of the average run lengths
ATS	Average time to signal
ATS(0)	In-control average time to signal
ATS(δ)	Out-of-control average time to signal
AATS	Average of the average time to signal
AATS(0)	In-control average of the average time to signal
AATS(δ)	Out-of-control average of the average time to signal
SDTS	Standard deviation of the time to signal
SDTS(0)	In-control standard deviation of the time to signal
SDTS(δ)	Out-of-control standard deviation of the time to signal
SDATS	Standard deviation of the average time to signal
SDATS(0)	In-control standard deviation of the average time to signal
SDATS(δ)	Out-of-control standard deviation of the average time to signal
EATS	Expected average time to signal
ANOS	Average number of observations to signal

ANOS(0)	In-control average number of observations to signal
ANOS(δ)	Out-of-control average number of observations to signal
AANOS	Average of the average number of observations to signal
AANOS(0)	In-control average of the average number of observations to signal
AANOS(δ)	Out-of-control average of the average number of observations to signal
SDANOS	Standard deviation of the average number of observations to signal
SDANOS(0)	In-control standard deviation of the average number of observations to signal
SDANOS(δ)	Out-of-control standard deviation of the average number of observations to signal
EAANOS	Expected average of the average number of observations to signal
ASI	Average sampling interval
ASS	Average sample size
ASS(0)	In-control average sample size
ASS(δ)	Out-of-control average sample size
ASS ₂	Two stage adaptive sample size
ASS ₃	Three stage adaptive sample size
FSI	Fixed sampling interval
FSS	Fixed sample size
pdf	Probability density function
cdf	Cumulative distribution function
icdf	Inverse cumulative distribution function
CL	Center line
UCL	Upper control limit
UWL	Upper warning limit
LCL	Lower control limit
LWL	Lower warning limit
CUSUM	Cumulative sum

CV	Coefficient of variation
DS	Double sampling
TS	Triple sampling
EWMA	Exponentially weighted moving average
SAS	Statistical analysis software
SPC	Statistical process control
SPM	Software process management
SQC	Statistical quality control
VSI	Variable sampling interval
VSS	Variable sample size
VSSI	Variable sample size and sampling interval
SPRT	Sequential probability ratio test
AI	Auxiliary information
RS	Run Sum
tpm	Transition probability matrix

LIST OF NOTATIONS

\bar{X}	Sample mean
S^2	Sample variance
T_i	Plotting statistic of the RS t and VSI RS t_K chart
\hat{T}_i	Plotting statistic of the VSI RS t_E chart
Y_{1i}, \bar{X}_{1i}	Mean of the first sample
\bar{X}_{2i}	Mean of the second sample
\bar{X}_{3i}	Mean of the third sample
Y_{2i}	Combined sample mean of the first and second samples
Y_{3i}	Combined sample mean of the first, second and third samples
W_{1i}	Charting statistic of the triple sampling \bar{X} chart at inspection level 1
W_{2i}	Charting statistic of the triple sampling \bar{X} chart at inspection level 2
W_{3i}	Charting statistic of the triple sampling \bar{X} chart at inspection level 3
n	Desired value of the average sample size of the adaptive sample size \bar{X} charts at each inspection level when the process is in-control; or fixed sample size of the FSS and adaptive sampling interval charts
m	Number of in-control Phase-I samples
μ_0	In-control population mean
μ_1	Out-of-control population mean
σ_0	In-control population standard deviation
$\hat{\mu}_0$	Estimator of the in-control population mean
$\hat{\sigma}_0$	Estimator of the in-control population standard deviation
I	Identity matrix
$\mathbf{1}$	Vector where all of its elements are ones
\mathbf{B}	Initial state/steady state probability vector
\mathbf{d}	Vector of sampling intervals
λ	Smoothing constant of the EWMA chart

δ	Size of a standardized mean shift
$\phi(\cdot)$	pdf of the standard normal random variable
$\Phi(\cdot)$	cdf of the standard normal random variable
t_0	Desired value of the average sampling interval
t_1	Short sampling interval for the VSI RS t chart
t_2	Long sampling interval for the VSI RS t chart
n_1	Smallest sample size for the adaptive sample size charts; or size of sample 1 at inspection level 1 of the DS/TS \bar{X} chart
n_2	Largest sample size for the ASS ₂ \bar{X} chart; or medium sample size for the ASS ₃ \bar{X} chart; or size of sample 2 at inspection level 2 of the DS/TS \bar{X} chart
n_3	Largest sample size for the ASS ₃ \bar{X} chart; or size of sample 3 at inspection level 3 of the TS \bar{X} chart
L_{11}, L_{12}	Limits of the DS/TS \bar{X} charts at inspection level 1
L_2	Limit of the DS \bar{X} chart at inspection level 2
L_{21}, L_{22}	Limits of the TS \bar{X} chart at inspection level 2
L_3	Limit of the TS \bar{X} chart at inspection level 3
$+S_a$	Score for the a^{th} region above the center line of the RS t /VSI RS t_K /VSI RS t_E chart
$-S_a$	Score for the a^{th} region below the center line of the RS t /VSI RS t_K /VSI RS t_E chart
R_a	a^{th} region above the center line of the RS t /VSI RS t_K chart
R_{-a}	a^{th} region below the center line of the RS t /VSI RS t_K chart
\hat{R}_a	a^{th} region above the center line of the VSI RS t_E chart
\hat{R}_{-a}	a^{th} region below the center line of the VSI RS t_E chart
P_a	Probability that the charting statistic of the RS t /VSI RS t_K chart falls in the a^{th} region above the center line
P_{-a}	Probability that the charting statistic of the RS t /VSI RS t_K chart falls in the a^{th} region below the center line

\hat{P}_a	Probability that the charting statistic of the VSI RS t_E chart falls in the a^{th} region above the center line
\hat{P}_{-a}	Probability that the charting statistic of the VSI RS t_E chart falls in the a^{th} region below the center line
$Q_{RS t}$	tpm of the RS t chart for the transient states
$Q_{\text{VSI EWMA } t}$	tpm of the VSI EWMA t chart for the transient states
Q_{ASS_2}	tpm of the ASS ₂ \bar{X} chart for the transient states
Q_{ASS_3}	tpm of the ASS ₃ \bar{X} chart for the transient states
$\hat{Q}_{\text{VSI RS } t_E}$	tpm of the VSI RS t_E chart for the transient states
$Q_{\text{VSI RS } t_K}$	tpm of the VSI RS t_K chart for the transient states
Y_i	Plotting statistic of the VSI EWMA t chart
$M_{(\text{RS } t)}$	Control limit coefficient of the RS t chart
$M_{(\text{VSI EWMA } t)}$	Control limit coefficient of the VSI EWMA t chart
$M_{(\text{VSI RS } t_K)}$	Control limit coefficient of the VSI RS t_K chart
$M_{(\text{VSI RS } t_E)}$	Control limit coefficient of the VSI RS t_E chart
l	Inspection level of the DS/TS \bar{X} chart
τ_1	Desired in-control ATS(0) value
τ_2	Desired in-control AATS(0) value
τ_3	Desired in-control ANOS(0) value
τ_4	Desired in-control ARL(0) value
τ_5	Desired in-control AANOS(0) value
τ_6	Desired in-control AARL(0) value
w	Warning limit coefficient of the VSI EWMA t chart
$+w^*$	Upper threshold (warning) limit of the ASS ₂ \bar{X} chart

$-w^*$	Lower threshold (warning) limit of the ASS ₂ \bar{X} chart
$+w_1, +w_2$	Upper threshold (warning) limits of the ASS ₃ \bar{X} chart
$-w_1, -w_2$	Lower threshold (warning) limits of the ASS ₃ \bar{X} chart
G	Positive integer used to control the switching between short and long sampling intervals for the RS t /VSI RS t_K /VSI RS t_E chart
TS_K	TS chart with known process parameters
TS_E	TS chart with estimated process parameters
DS_K	DS chart with known process parameters
DS_E	DS chart with estimated process parameters
t_K	t chart with known process mean
t_E	t chart with estimated process mean
$X_{li,j}$	j^{th} observation of inspection level l at sampling stage i for the DS/TS \bar{X} chart
$f_\gamma(\cdot)$	pdf of the gamma distribution
P_a	Probability of declaring a process as in-control for the DS/TS \bar{X} chart with known process parameters
P_{al}	Probability of declaring a process as in-control at inspection level l of the DS/TS \bar{X} chart with known process parameters
P_2	Probability of taking the second sample for the DS/TS \bar{X} chart with known process parameters
P_3	Probability of taking the third sample for the TS \bar{X} chart with known process parameters
\hat{P}_a	Probability of declaring a process as in-control for the DS/TS \bar{X} chart with estimated process parameters
\hat{P}_{al}	Probability of declaring a process as in-control at inspection level l of the DS/TS \bar{X} chart with estimated process parameters
\hat{P}_2	Probability of taking the second sample for the DS/TS \bar{X} chart with estimated process parameters
\hat{P}_3	Probability of taking the third sample for the TS \bar{X} chart with estimated process parameters

**PEMBANGUNAN CARTA HASILTAMBAH LARIAN SELANG PENSAMPELAN
BOLEH BERUBAH t DAN CARTA PENSAMPELAN BERGANDA TIGA \bar{X}
DENGAN PARAMETER PROSES YANG DIANGGARKAN**

ABSTRAK

Carta kawalan Shewhart \bar{X} adalah carta yang berguna dalam pemantauan proses. Walau bagaimanapun, prestasi carta Shewhart \bar{X} terjejas dengan ketara jika sisihan piawai proses dianggarkan dengan salah. Untuk mengatasi masalah ini, carta t biasanya digunakan sebagai alternatif kepada carta Shewhart \bar{X} . Objektif pertama dan kedua tesis ini bertujuan untuk meningkatkan prestasi carta t asas dengan mencadangkan carta-carta hasiltambah larian selang pensampelan boleh berubah (VSI RS) t bagi pemantauan min untuk proses yang bertaburan normal, masing-masing berdasarkan min proses yang diketahui dan dianggarkan. Teknik rantaian Markov digunakan untuk mengira parameter optima carta-carta baharu. Kepekaan carta VSI RS t dengan min proses diketahui yang dicadangkan adalah dinilai dan dibandingkan dengan carta-carta RS t dan VSI purata bergerak berpemberat eksponen (EWMA) \bar{X} sedia ada, dari segi kriteria masa purata untuk berisyarat (ATS) dan sisihan piawai masa untuk berisyarat (SDTS). Walau bagaimanapun, untuk carta VSI RS t dengan min proses yang dianggarkan, kriteria ATS purata (AATS) digunakan untuk menilai prestasi carta tersebut. Keputusan yang diperoleh menunjukkan bahawa carta VSI RS t dengan min proses diketahui yang dicadangkan pada amnya mengungguli carta-carta RS t and VSI EWMA t sedia ada dalam pengesanan anjakan min. Tambahan pula, prestasi AATS carta VSI RS t dengan min proses yang dianggarkan dinilai dengan menggunakan kriteria sisihan piawai ATS. Bilangan minimum sampel Fasa-I yang

diperlukan dalam anggaran min proses supaya carta VSI RS t dengan min proses yang dianggarkan mempunyai prestasi AATS dalam kawalan yang dikehendaki diberikan. Tambahan kepada dua objektif di atas, objektif ketiga tesis ini adalah untuk menunjukkan ralat dalam formula untuk mengira panjang larian purata (ARL) carta pensampelan berganda tiga (TS) \bar{X} berdasarkan parameter proses diketahui yang dicadangkan oleh He et al. pada tahun 2002 dan kemudiannya memberikan formula yang betul untuk pengiraan ARL carta tersebut. Versi carta TS \bar{X} yang betul dikenali sebagai carta TS \bar{X} dibaiki. Carta TS \bar{X} dibaiki dibandingkan dengan carta-carta pensampelan berganda dua (DS) \bar{X} , saiz sampel adaptif dua peringkat \bar{X} dan saiz sampel adaptif tiga peringkat \bar{X} apabila parameter proses adalah diketahui, dari segi kriteria ARL dan bilangan cerapan untuk berisyarat purata (ANOS). Analisis berangka menunjukkan bahawa carta TS \bar{X} dibaiki dengan parameter proses yang diketahui mengatasi prestasi carta DS \bar{X} yang sepadan dalam pengesanan kebanyakan saiz anjakan dalam min proses. Dalam perbandingan dengan carta $ASS_3 \bar{X}$ dan $ASS_2 \bar{X}$, carta TS \bar{X} dibaiki dengan parameter proses yang diketahui mengungguli dalam pengesanan semua saiz anjakan daripada segi kriteria ARL. Objektif keempat tesis ini adalah untuk membangunkan carta TS \bar{X} dibaiki dengan parameter proses yang dianggarkan dan membandingkan prestasinya dengan carta DS \bar{X} berdasarkan parameter proses yang dianggarkan melalui penggunaan kriteria ARL purata, sisihan piawai ARL, ANOS purata (AANOS) dan sisihan piawai ANOS (SDANOS), yang mana carta TS \bar{X} dibaiki dengan parameter proses yang dianggarkan didapati mengungguli carta DS \bar{X} dengan parameter proses yang dianggarkan. Tambahan pula, jadual yang memberikan bilangan minimum sampel Fasa-I untuk menganggarkan parameter proses supaya carta TS \bar{X} dibaiki dengan parameter proses yang dianggarkan mempunyai prestasi AARL dan AANOS dalam kawalan yang

dikehendaki diberikan. Pelaksanaan semua carta yang dicadangkan dijelaskan dengan menggunakan contoh kehidupan sebenar.

**DEVELOPMENT OF VARIABLE SAMPLING INTERVAL RUN SUM t CHART
AND TRIPLE SAMPLING \bar{X} CHART WITH ESTIMATED PROCESS
PARAMETERS**

ABSTRACT

The Shewhart \bar{X} control chart is a useful chart in process monitoring. However, the Shewhart \bar{X} chart's performance is significantly affected if the process standard deviation is erroneously estimated. To circumvent this problem, the t chart is commonly used as an alternative to the Shewhart \bar{X} chart. The first and second objectives of this thesis aim at enhancing the performance of the basic t chart by proposing the variable sampling interval run sum (VSI RS) t charts for monitoring the mean of a process from a normal distribution, based on known and estimated process mean, respectively. The Markov chain technique is used to compute the optimal parameters for the new charts. The sensitivity of the proposed VSI RS t chart with known process mean is evaluated and compared with the existing RS t and VSI exponentially weighted moving average (EWMA) t charts, in terms of the average time to signal (ATS) and standard deviation of the time to signal (SDTS) criteria. However, for the VSI RS t chart with estimated process mean, the average of the ATS (AATS) criterion is used in evaluating the chart's performance. The results obtained show that the proposed VSI RS t chart with known process mean generally outperforms the existing RS t and VSI EWMA t charts in detecting a mean shift. Additionally, the AATS performance of the VSI RS t chart with estimated process mean is assessed using the standard deviation of the ATS criterion. The minimum number of Phase-I samples required in estimating the process mean so that the VSI RS t chart with

estimated process mean has a desired in-control AATS performance is provided. In addition to the above two objectives, the third objective of this thesis is to point out the oversight in the formulae for computing the average run length (ARL) of the known process parameters based triple sampling (TS) \bar{X} chart proposed by He et al. in 2002, and then provide the correct formulae for the chart's ARL computation. The corrected version of the TS \bar{X} chart is called the revised TS \bar{X} chart. The revised TS \bar{X} chart is compared with the double sampling (DS) \bar{X} , two stage adaptive sample size \bar{X} and three stage adaptive sample size \bar{X} charts when process parameters are known, in terms of the ARL and average number of observations to signal (ANOS) criteria. The numerical analyses show that the revised $TS_K \bar{X}$ chart outperform the $DS_K \bar{X}$ chart, in the detection of most sizes of shifts in the process mean. In comparison with the $ASS_3 \bar{X}$ and $ASS_2 \bar{X}$ charts, the revised $TS_K \bar{X}$ chart prevails in detecting all shift sizes, in terms of the $ARL(\delta)$ criterion. The fourth objective of this thesis is to develop the revised TS \bar{X} chart with estimated process parameters and compare its performance with the estimated process parameters based DS \bar{X} chart using the average of the ARL, standard deviation of the ARL, average of the ANOS (AANOS) and standard deviation of the ANOS (SDANOS) criteria, where the estimated process parameters based revised TS \bar{X} chart is found to outperform the estimated process parameters based DS \bar{X} chart. Additionally, tables giving the minimum number of Phase-I samples for estimating the process parameters so that the revised TS \bar{X} chart with estimated process parameters has the desired in-control AARL and AANOS performances are provided. The implementations of all the proposed charts are explained using real life examples.

CHAPTER 1

INTRODUCTION

1.1 Quality and Statistical Process Control

The twenty first century is a period of globalization and fourth industrial revolution. The barriers to international trade and capital mobility have significantly being removed, which made the world more competitive. Manufacturing firms or industries have been playing enormous role in raising economic growth, enhancing economic development and expanding businesses and trades since the beginning of the industrial revolution. In this century, due to global liberalization, firms and industries are constrained by more challenges and competitions in setting prices and quality of their products as buyers or consumers want to purchase quality goods at lower prices. Therefore, it is highly required that firms or industries make serious attempts to ensure the quality of their products, in order to satisfy consumers' desires in this competitive market. Thus, quality plays a key built-in feature of a firm or company. The word quality represents the usefulness of a product in meeting one's needs and requirements. In an industry, a quality product refers to the fitness of the product for use that meets the expectations and necessities of the buyers. However, there exists an inverse proportional relationship between quality and variability. This implies that the quality of a product can be increased by reducing variability in the significant features of the product. The reduction of instability in the process and product contributes to the concept of quality enhancement.

Statistical Process Control (SPC) refers to a set of statistical tools used to improve the process by reducing variability in the key factors during the production cycle. SPC enables the production of higher quality and homogenous products with minimal defects, hence, resulting in less scrap. By implementing SPC, a significant

decrease in machine downtime, an increase in earning, an overall reduction in the cost of production, an increase in labour satisfaction, and an enhancement in the competitive position of an industry can all be attained (Smith, 1998).

Organizations around the world incorporate SPC as a key tool to improve product quality by reducing inevitable variations in the process. The inevitable variations in the process are categorized into two types: (1) random or common causes of variation and (2) assignable causes of variation. When the manufacturing process is running, the unavoidable “random or common causes” of variation is inherent in the process. In the presence of “random or common causes” of variation, the process continues to remain stable. This process is deemed as “in statistical control” or “in-control”. The assignable causes of variation, on the other hand, occurs due to the identifiable process disturbances, which can be detected and eliminated from the process. Faulty raw materials, operator mistakes and improper machine adjustments are examples of assignable causes of variation (Montgomery, 2019). If a manufacturing process operates with assignable causes of variation, the process is said to be unstable and therefore, is “out of statistical control” or “out-of-control”.

The advantages of adopting SPC include (1) the ability to maintain the consistency of the process and (2) the ability to assess quickly if changes occur due to causes other than random variability. If changes are detected through an investigation of the process, it is necessary to take appropriate corrective measures before additional defective products are being produced. Statistical tools are used in SPC to facilitate the detection of assignable causes of variation for elimination to improve process performance and maintain product quality. In SPC, tools like flowchart, Pareto chart, check sheet, cause-and-effect diagram, histogram, scatter diagram and control chart, are used to detect the anomalous process variability to attain quality enhancement. Those

tools have the ability to detect the assignable causes that create abnormal variability in the process which leads to errors and poor quality. In the pursuit of quality improvement in products manufactured and services rendered, SPC can be adopted by organizations.

1.2 Control Charts

Among the various statistical process monitoring tools in SPC, control chart is a useful process monitoring tool used in production and service processes to establish a stable and consistent operation. The idea of a control chart was introduced by Walter A. Shewhart in 1924 to monitor changes in the process over time when he was employed by the Bell Telephone Laboratories (Montgomery, 2019). A control chart plots the key product attributes in a time-ordered sequence to make decisions. The decision lines on a control chart are the 3-sigma upper control limit (UCL), central line (CL) and 3-sigma lower control limit (LCL). These decision lines are chosen to detect an out-of-control signal (Ryan, 2011). The idea behind the control chart is to select samples of the product from the production line periodically, then an inspector measures the drawn samples and computes the corresponding control chart's statistics, followed by plotting the chart's statistics on the aforementioned control chart, in order to detect variability in the production process over time.

Control charts can be constructed using two different types of data, namely, continuous data and attribute data. Control charts for continuous and attribute data are called variables and attribute control charts, respectively. Continuous data comprise continuous values that result from the numerical measurements of the quality characteristic. A variable control chart ensures practitioners a continuous quality improvement of the production by reducing the process variation (Gitlow et al., 1995).

Examples of quality characteristics having continuous data are the measurements of the diameter of piston rings in millimetres, board thickness in inches, flow width measures in millimetres, etc., which can all be measured numerically and monitored by the common variables control charts, such as the $\bar{X} - R$ and $\bar{X} - S$ charts. On the contrary, attribute control charts, like p , np , c and u charts plot the quality characteristics that are in the form of attribute data or discrete counts. The counts data are grouped as conforming or non-conforming, successful or unsuccessful, perfect or imperfect, and so forth. Practitioners adopt this kind of control charts to achieve a process without any defective items (Gitlow et al., 1995). Examples of data with discrete counts include the number of defective parts in the production of computers, office automation equipment, automobiles and the major subsystems of these products. In variables control charts, the data are plotted on a continuous scale and thus, they provide more information about measures of central tendency and variability. Therefore, variables charts are often more preferable than attribute charts.

An indispensable assumption in the construction of traditional control charts for process monitoring is that samples with a fixed size are taken at fixed sampling intervals, irrespective of the condition of the process. However, there are many circumstances in practice where practitioners need to vary the process parameters. In SPC, if the parameters of a control chart are allowed to vary when there is a signal of a change in the process, the chart is called an adaptive chart. Adaptive charts involve sampling at a higher rate, and thus, process changes can be detected quicker in comparison to traditional charts.

Process monitoring using control charts is conducted in two phases, namely, Phase-I (referred to as the retrospective phase) and Phase-II (referred to as the prospective phase). In Phase-I, historical data are studied to aid practitioners in

understanding the process and to assess the stability of the process, in ensuring that the process meets the intended target in the presence of only natural causes of variation. Then an in-control sample or reference sample is collected from this phase. Once an in-control reference sample is taken, the unknown process parameters are estimated from this sample so that the control limits for monitoring of the process in a future production can be computed. Additional discussions on Phase-I analysis can be found in Chakraborti et al. (2008) and Jones-Farmer et al. (2014). In Phase-II, control charts are implemented in order to monitor sudden changes in the process due to shifts and trends that occur in the process parameters so that the necessary corrective actions can be taken rapidly. Since the control limits in Phase-II are computed using the estimates from Phase-I, the success in prospectively monitoring the process in Phase-II is dependent on the accuracy of the Phase-I analysis.

1.3 Problem Statements

The Shewhart \bar{X} chart is usually used in process monitoring in manufacturing and service industries to enhance product quality. However, the Shewhart \bar{X} chart's performance is significantly affected if the process standard deviation is inaccurately estimated. To circumvent this setback, the basic t and EWMA t charts were proposed by Zhang et al. (2009), where the computations of the control limits of the said charts do not depend on the process standard deviation. The basic t and EWMA t charts are more robust against errors in estimating the process standard deviation than the \bar{X} and EWMA \bar{X} charts, respectively. Moreover, the run sum (RS) t chart was proposed by Sitt et al. (2014).

Research has shown that incorporating the variable sampling interval (VSI) technique into a control chart at hand can boost the efficiency of the latter (see Chew et al., 2015; Saha et al., 2019b; Nguyen et al., 2020; Ng et al., 2020; Teoh et al., 2021;

Sabahno et al., 2021; to name a few). Motivated by the need to further improve the performance of the RS t chart, the VSI technique proposed by Reynolds et al. (1988) will be integrated into the RS t chart in developing the VSI RS t chart to enhance the sensitivity of the RS t chart in detecting shifts in the process mean. This is the first objective in Section 1.4.

Usually, control charts are designed by assuming that the process parameters are known. However, in most process monitoring situations in practice, the process parameters are usually unknown and need to be estimated from an in-control Phase-I dataset. When the unknown process parameters are replaced by their estimates, the performance of a control chart will be significantly affected because of the variability in the estimation of process parameters. An accurate estimation of process parameters in Phase-I is crucial for the computation of reliable control limits for use in Phase-II process monitoring. In light of this importance, the estimated process parameter based VSI RS t chart will be developed in this thesis and this is the second objective in Section 1.4.

Another adaptive technique in improving the double sampling (DS) \bar{X} chart's performance is the triple sampling (TS) \bar{X} chart proposed by He et al. (2002). The TS \bar{X} chart shows superior performance to the DS \bar{X} chart proposed by Daudin (1992). However, the formula presented in He et al. (2002) for computing the average run length (ARL) value of the TS \bar{X} chart was incorrect. To circumvent this problem, the third objective in Section 1.4 deals with deriving new formulae for the design of the TS \bar{X} chart with known process parameters. Additionally, as the TS \bar{X} chart with estimated process parameters is not available in the literature, the fourth objective of this thesis is to develop the TS \bar{X} chart with estimated process parameters.

1.4 Objectives of the Thesis

The main objectives of this thesis are as follows:

- (i) To develop the known process parameter based VSI RS t chart by incorporating the variable sampling interval (VSI) technique into the run sum (RS) t chart.
- (ii) To develop the estimated process parameter based VSI RS t chart for monitoring the process mean.
- (iii) To derive new formulae for evaluating the performances of the triple sampling (TS) \bar{X} chart, in order to correct the oversight in the mathematical model of He et al. (2002).
- (iv) To develop the estimated process parameters based TS \bar{X} chart for monitoring the process mean.

1.5 Organization of the Thesis

There are seven chapters in this thesis. Chapter 1 provides a comprehensive overview of quality and SPC, as well as the problem statements and objectives of this study.

Chapter 2 covers a short description on the performance measures of the proposed control charts with known and estimated process parameters. A literature review on non-adaptive and adaptive charts are included in this chapter. The non-adaptive chart is the run sum t chart, while the adaptive charts are the VSI EWMA t , known and estimated process parameters based double sampling \bar{X} , two stage and three stage adaptive sample size \bar{X} and triple sampling \bar{X} charts.

Chapter 3 presents a new VSI RS t chart with known process parameter. The construction of the VSI RS t chart with known process parameter, its optimal design procedure and a performance comparison with competing charts are also explained in

this chapter. In addition, an example of application is given at the end of this chapter to facilitate the implementation of the VSI RS t chart with known process parameter.

Chapter 4 discusses the proposed estimated process parameter based VSI RS t chart and its performance measures. The construction and optimal design procedure of the said chart are described. The performance of the VSI RS t chart with estimated process parameter is compared with that of its known process parameter based counterpart. Furthermore, an example is presented to explain the implementation of the VSI RS t chart with estimated process parameter.

In Chapter 5, the error in the formulae of the performance measure of the TS \bar{X} chart with known process parameters, as reported in He et al. (2002), is pointed out. In addition, new formulae for the correct computations of the chart's performance measures are provided. The implementation procedure of the TS \bar{X} chart is explained. The construction and optimal design procedures of the TS \bar{X} chart with known process parameters adopting the new formulae, as well as the chart's performance evaluation are presented in this chapter. An example of application of the TS \bar{X} chart with known process parameters is demonstrated at the end of this chapter.

Chapter 6 explains the design of the TS \bar{X} chart when process parameters are estimated. The derivation of the statistical properties and the optimal designs of the aforesaid chart are also elaborated in this chapter. The performance of the TS \bar{X} chart with estimated process parameters is compared with that of the DS \bar{X} chart with estimated process parameters and the TS \bar{X} chart with known process parameters. In showing the application of the TS \bar{X} chart with estimated process parameters, this chapter ends with an illustrative example.

Chapter 7 summarizes the contributions and findings of this thesis. Recommendations for further research on related topics are also suggested in this chapter.

Optimization programs to compute the optimal parameters and values of the performance measures of all the charts proposed in this thesis are written in the MATLAB software and presented in Appendix A. Appendix B gives the simulation programs written in the Statistical Analysis Software (SAS) for verifying the results of the charts developed in this thesis, which are computed from the MATLAB programs in Appendix A. In the simulation programs, 20000 trials are used, as research shows that 20000 trials are sufficient to give accurate results (see Saha et al., 2022). The MATLAB optimization programs and SAS programs for the competing charts considered in this thesis are presented in Appendices C and D, respectively.

CHAPTER 2

A REVIEW ON PERFORMANCE MEASURES OF PROPOSED CHARTS, AND RELATED NON-ADAPTIVE AND ADAPTIVE CHARTS

2.1 Introduction

A control chart is known as a well designated chart when it has the ability in detecting shifts in the process rapidly and helps practitioners in taking corrective actions against producing defective products. The advantage of a Shewhart \bar{X} control chart is its simplicity of construction, thus, facilitating its implementation in manufacturing and service industries. However, the Shewhart \bar{X} control charting technique is not adequate in an advanced manufacturing environment as the Shewhart \bar{X} chart is slow in detecting small and moderate process shifts in the location and dispersion parameters. Furthermore, the performance of the Shewhart \bar{X} chart is highly affected by changes in the process standard deviation. The t type charts have been proposed to overcome the setback of the Shewhart \bar{X} chart which is affected by changes in the process standard deviation. Furthermore, in improving the performance of Shewhart charts, attention is devoted in developing adaptive type charts, in order to achieve a quicker detection of process shifts for a more effective process monitoring.

This chapter provides preliminaries and reviews of the run sum t and adaptive type charts that are related to the proposed charts discussed in Chapters 3, 4, 5 and 6. In Section 1.3 (Problem Statements), it is mentioned that the design of adaptive type control charts with known and estimated process parameters is useful and important in practice. Hence, several performance measures that are crucial in evaluating the performances of adaptive control charts with known and estimated process parameters are discussed in Section 2.2.

In Section 2.3, a review on run sum (RS) t chart that is related to objectives (i) and (ii) in Section 1.4 is given. Section 2.4 presents a review on adaptive type charts. The variable sampling interval (VSI) EWMA t chart which is also related to objective (i) in Section 1.4 is discussed in Section 2.4.1. The double sampling (DS) \bar{X} , two and three stage adaptive sample size \bar{X} , and triple sampling (TS) \bar{X} charts, which are related to objective (iii) in Section 1.4 are discussed in Sections 2.4.2 – 2.4.5. The DS \bar{X} chart with estimated process parameters which is related to objective (iv) in Section 1.4 is explained in Section 2.4.6.

2.2 Performance Measures of Control Charts

In SPC, the performance of a control chart is evaluated by how quickly the chart detects process changes. The process changes can occur in the mean or variance (or both) of the process. The statistical measures that are adopted in assessing a chart's performance are called the performance measures of control charts. Numerous types of performance measures are available in the literature of SPC. The performance measures considered in evaluating the performances of the proposed and competing charts in this thesis are the average run length (ARL), average time to signal (ATS), standard deviation of the time to signal (SDTS), average number of observations to signal (ANOS), average of the average time to signal (AATS), standard deviation of the average time to signal (SDATS), average of the average run lengths (AARL), standard deviation of the average run lengths (SDARL), average of the average number of observations to signal (AANOS) and standard deviation of the average number of observations to signal (SDANOS) criteria. When process parameters can be specified, the performances of non-adaptive charts can be studied using the ARL criterion (see Castagliola et al., 2017 and Ng et al., 2018), whereas the ATS, SDTS

and ANOS criteria can be used to study adaptive charts' performances (See Reynolds et al., 1988; Nguyen et al., 2020; Saha et al. 2019a; Motsepa et al., 2020 and Teoh et al., 2021). The AARL, SDARL, AATS, SDATS, AANOS and SDANOS criteria are used to study the performances of control charts when process parameters are estimated (Aparisi et al., 2018; Castagliola et al., 2017 and Saha et al., 2019b). The following sections provide explanations on the aforementioned performance measures.

2.2.1 Average Run Length

The average run length (ARL) measures the expected number of samples that needs to be plotted on a control chart before the first out-of-control signal is detected (Montgomery, 2019). The ARL can be classified as an in-control ARL ($ARL(0)$) or an out-of-control ARL ($ARL(\delta)$), where δ represents the standardized size of the process shift. In order to ensure a low false alarm rate, the $ARL(0)$ value should be large. On the contrary, the $ARL(\delta)$ value should be small in order to enable the process shifts to be detected quickly. A common practice in SPC is to compare the $ARL(\delta)$ values of the charts under comparison by specifying the same $ARL(0)$ value, for the said charts. Then the chart with the smallest $ARL(\delta)$ value is considered as superior to the other competing charts.

2.2.2 Average Time to Signal

The average time to signal (ATS) is the expected time needed by a chart to detect a process shift (Reynolds et al., 1988). This criterion is adopted to assess the performances of adaptive charts, such as the VSI, variable sample size and sampling interval (VSSI), and variable parameters (VP) charts by measuring the expected amount of time needed until the charts produce a signal. For a fixed sampling interval

(FSI) chart, the ATS value is a product of the chart's ARL and FSI values. The ATS is categorized as either in-control ($ATS(0)$) when the process is in-control or out-of-control ($ATS(\delta)$) when the process is out-of-control. When the process shifts, the chart with the smallest $ATS(\delta)$ value is deemed to have the best performance among the competing charts.

2.2.3 Standard Deviation of the Time to Signal

The standard deviation of the time to signal (SDTS) is computed together with the ATS to study the variation or spread in the time to signal distribution (Reynolds et al., 1988). The SDTS can be obtained for an in-control process and an out-of-control process as $SDTS(0)$ and $SDTS(\delta)$, respectively. A large value of SDTS implies a large variation in the time to signal distribution, while a small value of SDTS implies a small variability in the distribution of the time to signal. A control chart with a smaller SDTS value is considered as superior to its competing charts when a similar $ATS(0)$ value is set for all the charts.

2.2.4 Average Number of Observations to Signal

The average number of observations to signal (ANOS) counts the average number of observations needed until an out-of-control signal is detected (Khoo et al., 2015). The ANOS of a chart with a fixed sample size (FSS) is obtained by simply taking the product of the ARL and FSS values, while for adaptive charts, such as the VSS, VSSI and VP charts, it is obtained directly by counting the number of observations needed to trigger an out-of-control signal. Like the ARL and ATS values, the ANOS value can also be classified as either an in-control ANOS ($ANOS(0)$) value or an out-of-control ANOS ($ANOS(\delta)$) value, depending on the state of the process. The $ANOS(0)$

value denotes the average number of observations that is needed by a chart in issuing the first false alarm when the process is in-control, while the $ANOS(\delta)$ value is the average number of observations needed by a chart to produce an out-of-control signal when the process is off-target.

2.2.5 Average of the Average Run Lengths

The ARL is used in assessing the efficiency of control charts in detecting process shifts when process parameter(s) are known. When these process parameter(s) are unknown and estimated from different Phase-I samples, the ARL values computed vary from practitioner to practitioner. The average of these ARL values is called the average of the average run lengths (AARL) (Lee and Khoo., 2021). The in-control AARL ($AARL(0)$) and out-of-control AARL ($AARL(\delta)$) criteria are adopted in process monitoring. Like the other performance measures explained earlier, the chart with a smaller $AARL(\delta)$ value is superior to its competing charts.

2.2.6 Standard Deviation of the Average Run Lengths

The standard deviation of the average run lengths (SDARL) criterion measures the variation or spread in the computed ARL values) (Saha et al., 2017). When a limited number of Phase-I samples is used to estimate the unknown process parameters, the AARL value of the estimated process parameters based chart varies from that of the aforesaid chart's ARL value obtained by assuming known process parameters. Moreover, if the number of Phase-I samples used in the estimation of process parameters increase, the AARL value obtained for the estimated process parameters based chart will be closer to the ARL value of the chart's known process parameters counterpart, even though a considerable difference exists. Therefore, the SDARL

criterion helps practitioners to determine the minimum number of Phase-I samples needed in the estimation of process parameters so that the estimated process parameters based chart's AARL value is sufficiently closed to the ARL value of the chart's known process parameters counterpart. The in-control and out-of-control SDARL values are denoted as $SDARL(0)$ and $SDARL(\delta)$, respectively.

2.2.7 Average of the Average Time to Signal

For an estimated process parameters based chart, the computed ATS values of the chart vary from practitioner to practitioner when different Phase-I samples are used to estimate the unknown process parameters. The average of these ATS values is called the average of the average time to signal (AATS) (Saha et al., 2019b) value. The AATS criterion is used in assessing the efficiency of adaptive charts in detecting process shifts when process parameters are estimated. The in-control and out-of-control AATS are denoted as $AATS(0)$ and $AATS(\delta)$, respectively.

2.2.8 Standard Deviation of the Average Time to Signal

The standard deviation of the average time to signal (SDATS) criterion measures the variation or spread in the computed average time to signal values when process parameters are estimated) (Saha et al., 2019b). When a limited number of Phase-I samples is used to estimate the unknown process parameters, the AATS value of the estimated process parameters based chart varies from the ATS value of the aforesaid chart with known process parameters. Moreover, if the number of Phase-I samples used in the estimation of process parameters is increased, the AATS value of the chart with estimated process parameters will become closer to the ATS value of the corresponding chart with known process parameters although a considerable

difference still exists. Therefore, the SDATS criterion helps practitioners to determine the minimum number of Phase-I samples needed in estimating the process parameters so that the AATS value of the estimated process parameters based chart is sufficiently close to the ATS value of the chart's known process parameters counterpart. The in-control and out-of-control SDATS are denoted as $SDATS(0)$ and $SDATS(\delta)$, respectively.

2.2.9 Average of the Average Number of Observations to Signal

The average of the average number of observations to signal (AANOS) criterion is preferable over the ANOS criterion in evaluating the performance of control charts with estimated process parameters. As the Phase-I samples vary from practitioner to practitioner, in the estimation of process parameters, the ANOS behaves as a random variable. Therefore, the average of the ANOS values has to be computed and this average is the AANOS value. The in-control AANOS is denoted as $AANOS(0)$ and the out-of-control AANOS as $AANOS(\delta)$.

2.2.10 Standard Deviation of the Average Number of Observations to Signal

The standard deviation of the average number of observations to signal (SDANOS) criterion is used to study the variation in the values of the average number of observations to signal. When a small number of Phase-I observations is used to estimate the unknown process parameters, the AANOS value of the chart with estimated process parameters differs from the corresponding ANOS value of the chart's known process parameters counterpart. When the number of Phase-I samples in estimating the unknown process parameters increases, the AANOS value of the estimated process parameters based chart becomes closer to the ANOS value of the

chart's known process parameters based counterpart. The SDANOS criterion is used to determine the minimum number of in-control Phase-I samples needed to estimate the process parameters so that the AANOS value of the estimated process parameters based chart is sufficiently close to the ANOS value of the chart's corresponding known process parameters based counterpart.

2.3 Run Sum t Chart

The run sum (RS) chart is a powerful and efficient process monitoring tool as it provides a rapid detection of process shifts besides its ease of implementation. In the RS technique, the interval between the chart's upper and lower control limits is split into multiple regions or zones and a score is allocated to each region, hence, the RS chart is also called the zone chart. A control chart with the RS technique signals an out-of-control situation when the cumulative sum of the scores reaches or exceeds a predefined value, called the triggering score. Jaehn (1987) introduced the first zone chart, while Davis et al. (1990) modified it into an improved zone chart with a superb performance compared to the Shewhart chart with runs rules. To monitor the process mean, Champ and Rigdon (1997) proposed the RS \bar{X} chart which outperforms the \bar{X} chart. More recent researches on RS charts were made by Rakitzis and Antzoulakos (2016), Teoh et al. (2017) and Ng et al. (2018), to name some. A summary of existing studies on run sum charts are given in Table 2.1.

Assume that $X_{i,1}, X_{i,2}, \dots, X_{i,n}$ is the i^{th} random sample of size n , for $i = 1, 2, \dots$, taken from a process that follows the normal $N(\mu_0 + \delta\sigma_0, \gamma^2\sigma_0^2)$ distribution, where μ_0 and σ_0 are the in-control process mean and standard deviation, respectively. It is also assumed that the observations within and between the samples are independent. The process is in-control when $\delta = 0$ and $\gamma = 1$, otherwise, the process is out-of-control,

Table 2.1. A summary of existing run sum control charts and their descriptions

	Author(s)	Title and journal information	Description
1	Jaehn	Title: Zone control charts - SPC made easy Journal: <i>Quality</i> , 1987, 26(10), 51-53	A special case of run sum chart, named zone control chart was proposed. The interval between the chart's upper and lower control limits is divided into four regions.
2	Davis et al.	Title: Performance of the zone control chart Journal: <i>Communications in Statistics - Theory and Methods</i> , 1990, 19(5), 1581-1587	This study investigates the ARL properties of the zone control chart and compares its performance with that of the Shewhart charts with supplementary runs rules.
3	Champ and Rigdon	Title: An analysis of the run sum control chart Journal: <i>Journal of Quality Technology</i> , 1997, 29(4), 407-417	The run length distribution of the run sum \bar{X} chart using the Markov chain approach was presented, where this chart was found to outperform the \bar{X} chart.
4	Sitt et al.	Title: The run sum t control chart for monitoring process mean changes in manufacturing. Journal: <i>The International Journal of Advanced Manufacturing Technology</i> , 2014, 70(5-8), 1487-1504.	The RS technique was combined with the t chart to enhance the performance of the t chart in monitoring the process mean changes in manufacturing. The statistical design in minimizing the out-of-control ARL and the economic statistical design in minimizing the cost function were studied. The proposed RS t chart has outstanding performance compared with the basic t chart for all shift sizes. The RS t chart also outperforms the VSI EWMA t chart in detecting large and moderate shifts.
5	Rakitzis and Antzoulakos	Title: Run sum control charts for the monitoring of process variability. Journal: <i>Quality Technology & Quantitative Management</i> , 2016, 13(1), 58-77.	A two-sided run sum S control chart was introduced and its ARL performance is evaluated via a Markov chain approach.
6	Teoh et al.	Title: Run-sum control charts for monitoring the coefficient of variation. Journal: <i>European Journal of Operational Research</i> , 2017, 257(1), 144-158.	A simple yet efficient procedure for monitoring the coefficient of variation (CV) by adopting the run sum control charting technique was discussed. The run length properties of the run sum CV chart were analysed using the Markov chain approach. Two optimization techniques by minimizing the (i) ARL for a specified shift size and (ii) expected ARL over a process shift domain, were discussed. Numerical analyses show that the proposed RS CV charts outperform their existing counterparts for all or certain ranges of shifts in the CV.

as either δ , γ or both have changed. The sample mean, \bar{X}_i and sample variance, S_i^2 are computed from the i^{th} sample as

$$\bar{X}_i = \frac{1}{n} \sum_{j=1}^n X_{i,j} \quad (2.1)$$

and

$$S_i^2 = \frac{1}{n-1} \sum_{j=1}^n (X_{i,j} - \bar{X}_i)^2, \quad (2.2)$$

respectively.

The RS t chart (Sitt et al., 2014) is based on dividing the interval between the upper and lower control limits of the standard t chart into regions, with a regions, each above and below the center line (CL). The charting statistic of the RS t chart is

$$T_i = \frac{(\bar{X}_i - \mu_0)\sqrt{n}}{S_i}, \text{ for } i=1, 2, \dots, \quad (2.3)$$

where T_i follows the Student's t distribution with $n - 1$ degrees of freedom when the process is in-control, while T_i follows the non-central Student's t distribution with $n - 1$ degrees of freedom and non-centrality parameter $\delta\sqrt{n}/\gamma$ when the process is out-of-control. Note that in Equation (2.3), n denotes the sample size.

Figure 2.1 presents a graphical representation of the two-sided RS t chart. In Figure 2.1, there are a regions, each above and below the CL of the RS t chart. The a regions above the CL ($= 0$), i.e. R_1, R_2, \dots, R_a are allocated the scores $+S_1, +S_2, \dots, +S_a$, respectively, while the a regions below the CL, namely, $R_{-1}, R_{-2}, \dots, R_{-a}$ are allocated the scores $-S_1, -S_2, \dots, -S_a$, respectively. Additionally, the probability of T_i (for $i = 1, 2, \dots$) falling in the region R_r is denoted as P_r (i.e. $\Pr(T_i \in R_r) = P_r$), for $r = -a, -a + 1, \dots, -1, 1, 2, \dots, a - 1, a$.

The r^{th} upper and lower control limits, called UCL_r and LCL_r , respectively, of the RS t chart are computed as

$$UCL_r = M_{(RS\ t)} \times F_t^{-1}(\alpha_r), \text{ for } r = 1, 2, \dots, a - 1 \quad (2.4a)$$

and

$$LCL_r = -UCL_r, \quad (2.4b)$$

where $F_t^{-1}(\cdot)$ is the inverse cumulative distribution function (icdf) of the Student's t distribution with $n - 1$ degrees of freedom and

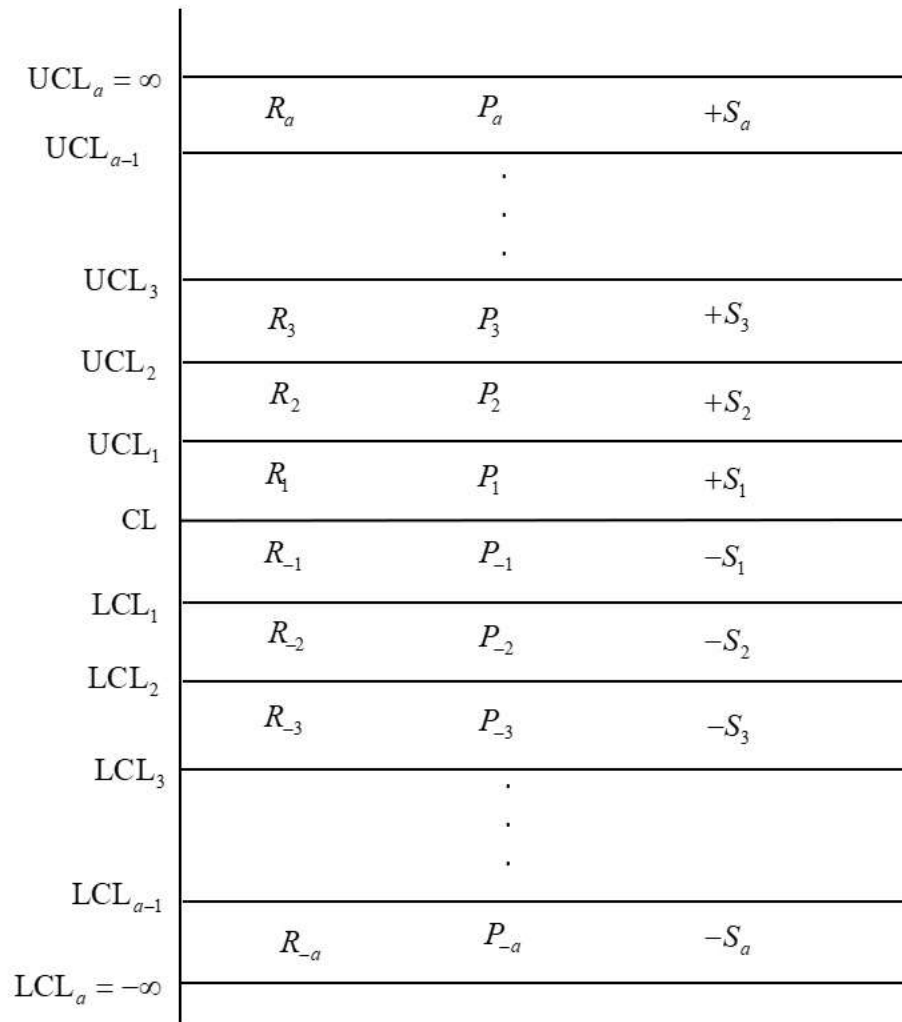


Figure 2.1. A graphical representation of the two-sided RS t chart with a regions, each above and below the CL

$$\alpha_r = \Phi\left(\frac{3r}{a-1}\right), \text{ for } r = 1, 2, \dots, a-1. \quad (2.5)$$

Here, $\Phi(\cdot)$ is the cumulative distribution function (cdf) of the standard normal distribution. The value of the parameter $M_{(RS\ t)}$ is chosen to attain a desired in-control performance for the RS t chart.

The r^{th} region above the CL is represented as

$$R_r = [\text{UCL}_{r-1}, \text{UCL}_r], \text{ for } r = 1, 2, \dots, a \quad (2.6a)$$

and that below the CL as

$$R_r = (\text{LCL}_r, \text{LCL}_{r-1}], \text{ for } r = 1, 2, \dots, a. \quad (2.6b)$$

In Equations (2.6a) and (2.6b), $\text{UCL}_0 = \text{LCL}_0 = \text{CL}$. The score function, $S(T_i)$, for $i = 1, 2, \dots$, is characterized as

$$S(T_i) = \begin{cases} +S_r & \text{if } T_i \in [\text{UCL}_{r-1}, \text{UCL}_r) \\ -S_r & \text{if } T_i \in (\text{LCL}_r, \text{LCL}_{r-1}] \end{cases}, \text{ for } r = 1, 2, \dots, a. \quad (2.7)$$

The RS t chart works based on the cumulative scores, U_i or L_i . If the cumulative score $U_i \geq +S_a$ or $L_i \leq -S_a$, the chart triggers an out-of-control signal. The cumulative scores U_i and L_i are defined in Equations (2.8a) and (2.8b), respectively.

$$U_i = \begin{cases} 0 & \text{if } T_i < \text{CL} \\ U_{i-1} + S(T_i) & \text{if } T_i \geq \text{CL} \end{cases}, \quad (2.8a)$$

and

$$L_i = \begin{cases} 0 & \text{if } T_i > \text{CL} \\ L_{i-1} + S(T_i) & \text{if } T_i \leq \text{CL} \end{cases}, \quad (2.8b)$$

for $i = 1, 2, \dots$, where the initial values of the RS t chart are set as $U_0 \geq 0$ and $L_0 \geq 0$.

If $U_0 = 0$ and $L_0 = 0$, the no head-start feature is used.

The ARL and SDRL values of the RS t chart for a standardized mean shift of size δ are computed as (Sitt et al., 2014)

$$\text{ARL}(\delta) = \mathbf{B}^T (\mathbf{I} - \mathbf{Q}_{\text{RS } t})^{-1} \mathbf{1} \quad (2.9)$$

and

$$\text{SDRL}(\delta) = \sqrt{2\mathbf{B}^T (\mathbf{I} - \mathbf{Q}_{\text{RS } t})^{-1} \mathbf{1} - (\text{ARL}(\delta))^2} + \text{ARL}(\delta), \quad (2.10)$$

where $\mathbf{B}^T = (1, 0, 0, \dots, 0)$ is the initial probability vector, $\mathbf{Q}_{\text{RS } t}$ is the transition probability matrix (tpm) of the Markov chain model for the transient states of the RS t chart, \mathbf{I} is an identity matrix and $\mathbf{1}$ is a column vector with all of its entries equal to unity. A step-by-step procedure for obtaining the tpm, $\mathbf{Q}_{\text{RS } t}$ is given in Sitt et al. (2014).

The ATS and SDTS values of the RS t chart are computed as

$$\text{ATS}(\delta) = \mathbf{B}^T (\mathbf{I} - \mathbf{Q}_{\text{RS } t})^{-1} \mathbf{d} \quad (2.11)$$

and

$$\text{SDTS}(\delta) = \sqrt{\mathbf{B}^T \mathbf{c}_2 - (\mathbf{B}^T \mathbf{c}_1)^2}, \quad (2.12)$$

where \mathbf{d} is a column vector with all of its entries equal to the FSI of the RS t chart, $\mathbf{c}_2 = (\mathbf{I} - \mathbf{Q}_{\text{RS } t})^{-1} (2\mathbf{C}_d \mathbf{b}_1 - \mathbf{d}^{(2)})$ and $\mathbf{c}_1 = (\mathbf{I} - \mathbf{Q}_{\text{RS } t})^{-1} \mathbf{d}$. Note that \mathbf{b}_1 is the value of the first element in \mathbf{B} . The vector $\mathbf{d}^{(2)}$ comprises the squares of the elements in vector \mathbf{d} , while \mathbf{C}_d is a diagonal matrix with its elements taken from the vector \mathbf{d} . The vector \mathbf{B} and matrices $\mathbf{Q}_{\text{RS } t}$ and \mathbf{I} have been defined prior to this discussion. The optimization programs written in the MATLAB software in minimizing the $\text{ATS}(\delta)$ value of the RS t chart are given in Appendix C.1.

2.4 Some Related Adaptive Type Charts

In general, the design of a control chart depends on three parameters, i.e. the sampling interval (t), sample size (n) and control limit coefficient (M). A control chart is an adaptive chart if at least one of its parameters is permitted to vary in real time based

on the actual values of the past sample statistics. When the sampling interval of a chart is allowed to vary, the chart is called a VSI chart. If the sample size of a chart is allowed to vary, the chart is called a VSS chart, while if the chart is allowed to vary both its sampling interval and sample size, it is called a VSSI chart. In addition, if all parameters of a chart are allowed to vary, the chart is known as a VP chart.

Tagaras (1998) presented a comprehensive review on the design of adaptive charts. It includes all types of adaptive charts that adopt the VSS, VSI and VP features. The DS \bar{X} and TS \bar{X} charts are adaptive charts, where the sample sizes vary according to the current process quality. A literature review on adaptive charts is elaborated hereafter.

Varying the sampling interval between two consecutive samples is the first technique on adaptive charts. Reynolds et al. (1988) proposed the VSI \bar{X} chart and found that this chart was substantially quicker than the FSI \bar{X} chart in detecting a process mean shift. Since then, the integration of the VSI technique with other types of control charts has been widely studied. Saccucci et al. (1992) proposed the VSI EWMA \bar{X} chart which outperforms the EWMA \bar{X} chart. Lee and Bai (2000) studied the run length properties of the VSI \bar{X} chart with runs rules. The monitoring of the process mean and variance using individual measurements via the VSI technique was suggested by Reynolds and Stoumbos (2001). Castagliola et al. (2013a) monitored the coefficient of variation (CV) using the VSI technique, where the proposed chart shows a considerable improvement in detecting changes in the CV. In order to increase the effectiveness of the sequential probability ratio test (SPRT) chart in detecting shifts in the process mean, Ou et al. (2011) integrated the VSI technique with the SPRT chart, where the VSI SPRT chart outperforms the SPRT chart. Kazemzadeh et al. (2013) introduced the VSI EWMA t chart by adding an additional warning limit to the EWMA

t chart proposed by Zhang et al. (2009). Ng et al. (2020) incorporated the auxiliary information (AI) and VSI techniques into the EWMA chart. Nguyen et al. (2020) combined the VSI strategy with the CUSUM technique to develop a new chart for monitoring the ratio of two variables. Furthermore, Haq and Akhtar (2020) discovered that the AI based maximum EWMA and maximum double EWMA charts with the VSI scheme have outstanding performances in detecting mean shifts. More recently, Tran et al. (2021) studied the effect of measurement errors on the performance of the VSI EWMA median chart.

A type of adaptive chart that has received a great deal of attention is the DS chart. The DS \bar{X} control charting technique was pioneered by Croasdale (1974), where a decision about the status of a process (in-control or out-of-control) depends on the information of the second sample. Daudin (1992) modified the Croasdale's DS \bar{X} procedure by using information from either the first sample or the combined samples in deciding about the status of the process. Irianto and Shinozaki (1998) presented an optimal design procedure for the DS \bar{X} chart, where the power of the chart in detecting shifts is maximized, instead of minimizing the average sample size (ASS). Carot et al. (2002) combined the VSI and DS \bar{X} techniques and showed that the new chart performs better than the DS \bar{X} chart. The economic design of the combined DS and VSI \bar{X} charts was studied by Lee et al. (2012). Haq and Khoo (2018) found that the auxiliary information based DS chart has a superb ARL performance compared to the basic DS chart. A chart based on the combined VSI, DS and AI techniques for tracking process mean shifts was proposed by Umar et al. (2020). Malela-Majika et al. (2021) developed a side sensitive DS \bar{X} chart which is superior to the basic DS \bar{X} chart.

The two stage adaptive sample size (ASS₂) modification of the Shewhart \bar{X} chart was introduced by Prabhu et al. (1993), where the proposed chart is significantly